SUPPLEMENTARY INFORMATIONS

Figure S1:

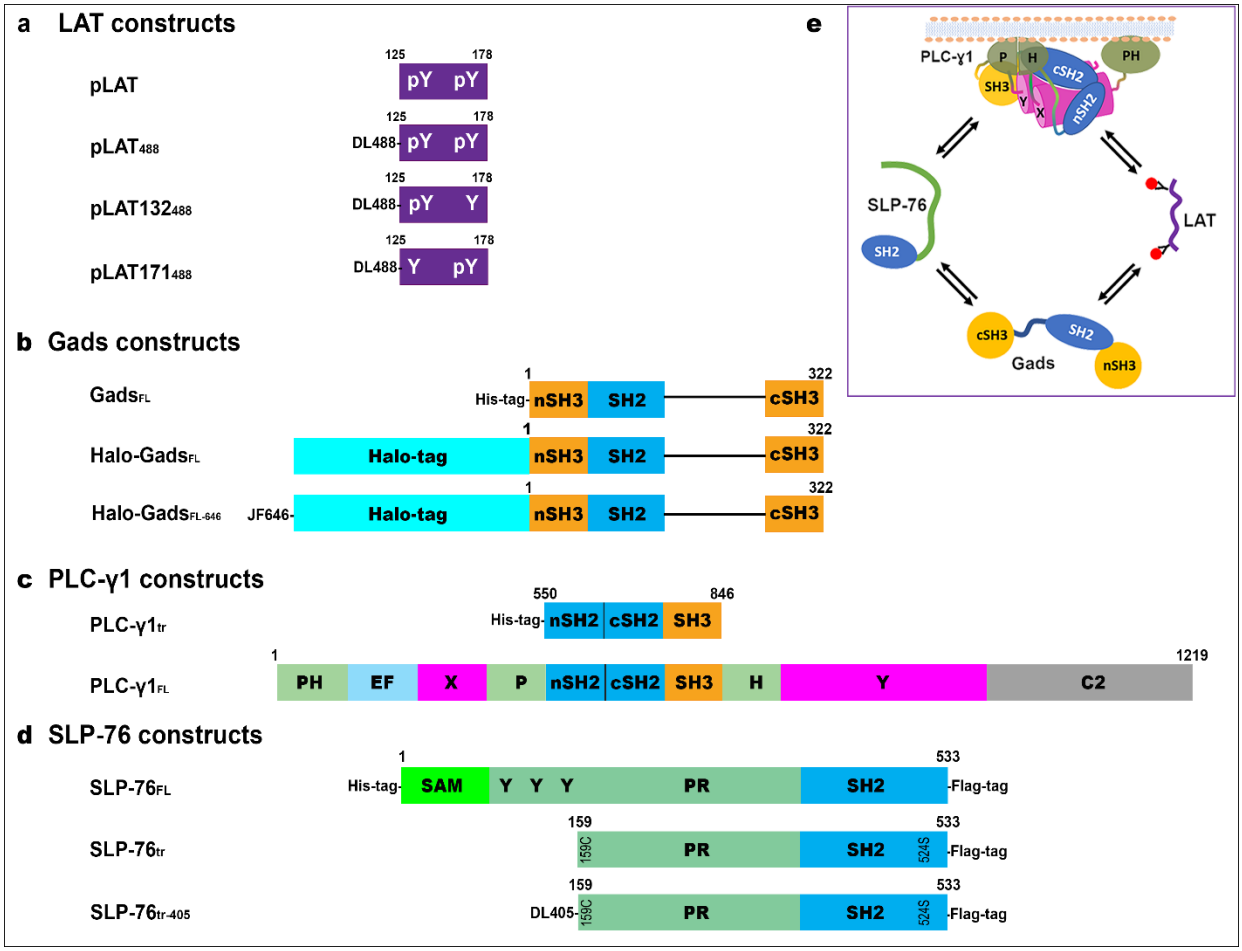

Figure S1: **Domain organization of the protein and peptide components, and their interactions.** Different domains are distinguished by color. Affinity tags and fluorophores are indicated in the corresponding domain structure. Labeled peptide or proteins are indicated by the corresponding fluorophore absorbance maxima number in the suffix. **a,** doubly phosphorylated pLAT, $pLAT_{488}$ and singly phosphorylated $pLAT132_{488}$, and $pLAT171_{488}$; **b,** $Gads_{FL}$, Halo-$Gads_{FL}$ and Halo-$Gads_{FL-646}$; **c,** PLC-$\gamma1_{tr}$ and PLC-$\gamma1_{FL}$; **d,** SLP-76_{FL}, SLP-76_{tr} and SLp-76_{tr-405}. **e,** Schematic showing mutual binding interfaces between the four proteins.

Figure S2:

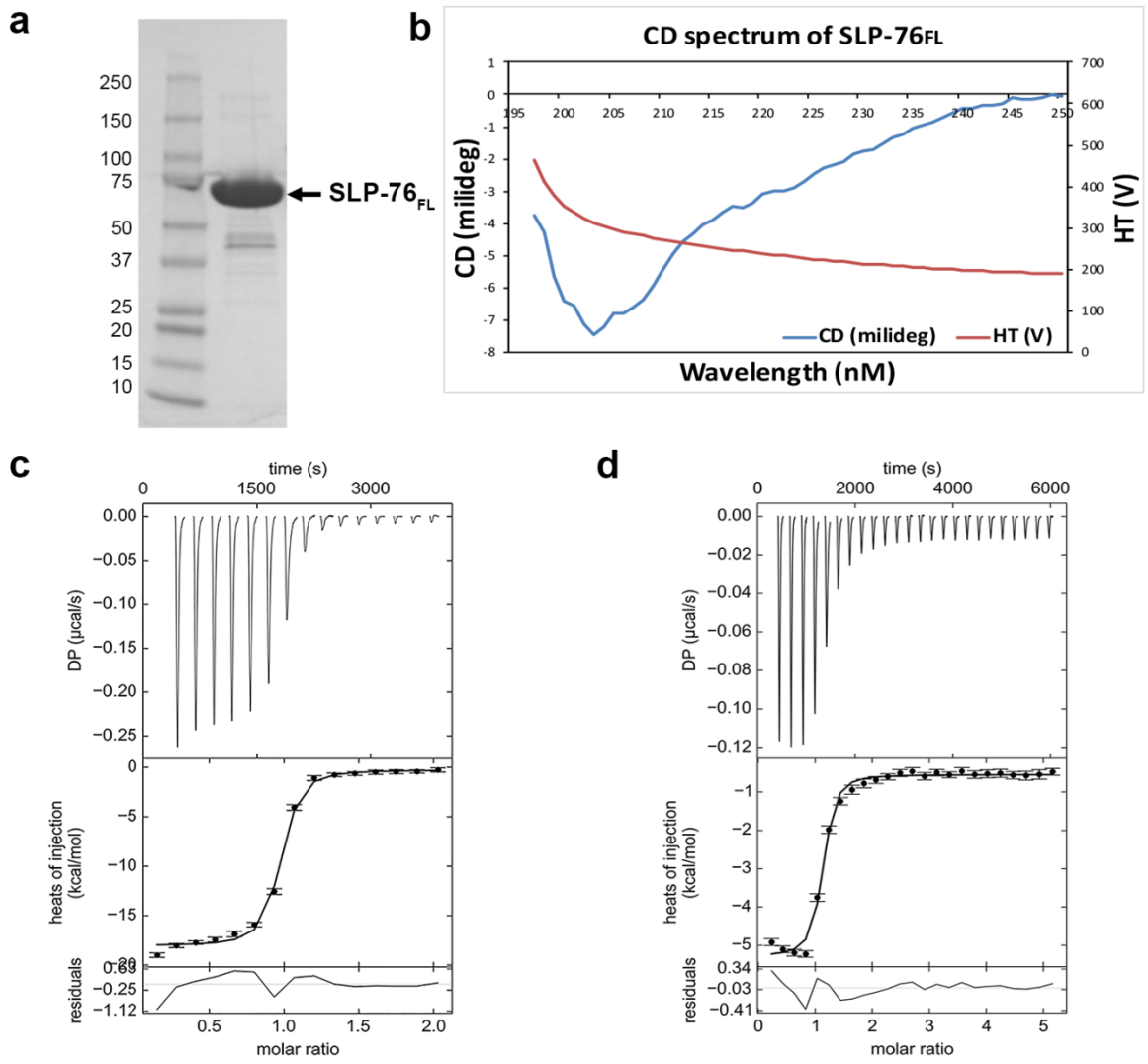

Figure S2: **Characterization of Full length SLP-76$_{FL}$ produced by overexpression in bacteria. a,** SDS-PAGE 4-15% gradient gel stained by Coomassie Blue. The arrow indicate SLP-76$_{FL}$. **b,** CD spectra (blue) and HT voltage (red) of SLP-76$_{FL}$ recorded with a Jasco-815 CD spectropolarimeter in PBS at room temperature. **c,** ITC binding isotherm for SLP-76$_{FL}$ (syringe) with full length GADS (cell). **d,** ITC binding isotherm for SLP-76$_{FL}$ (cell) with Phospho-HPK (pY381) peptide (syringe). ITC titrations were performed at 25°C in PBS.

Figure S3:

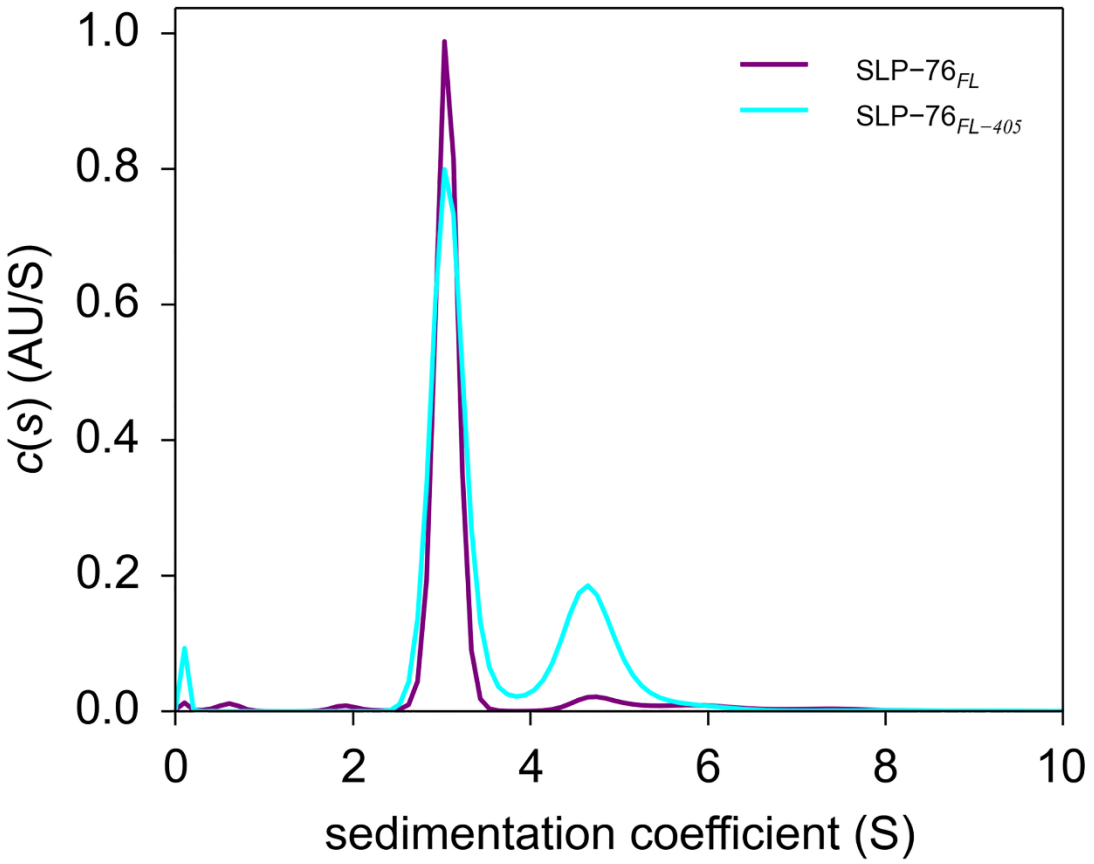

Figure S3: **Labeling of SLP-76$_{FL}$ with Dylight 405 NHS ester induces dimerization of SLP-76$_{FL}$.** In this preparation, a the population of dimeric SLP-76$_{FL}$ increased from less than 5% for unlableled protein to ≈30 % after chromophoric labeling. The c(s) distributions, obtained from 280 nm absorbance data, of SLP-76$_{FL}$ (purple) or its labeled form SLP-76$_{FL-405}$ (cyan) are superimposed and fraction of dimer were calculated from the area under the peaks.

Figure S4

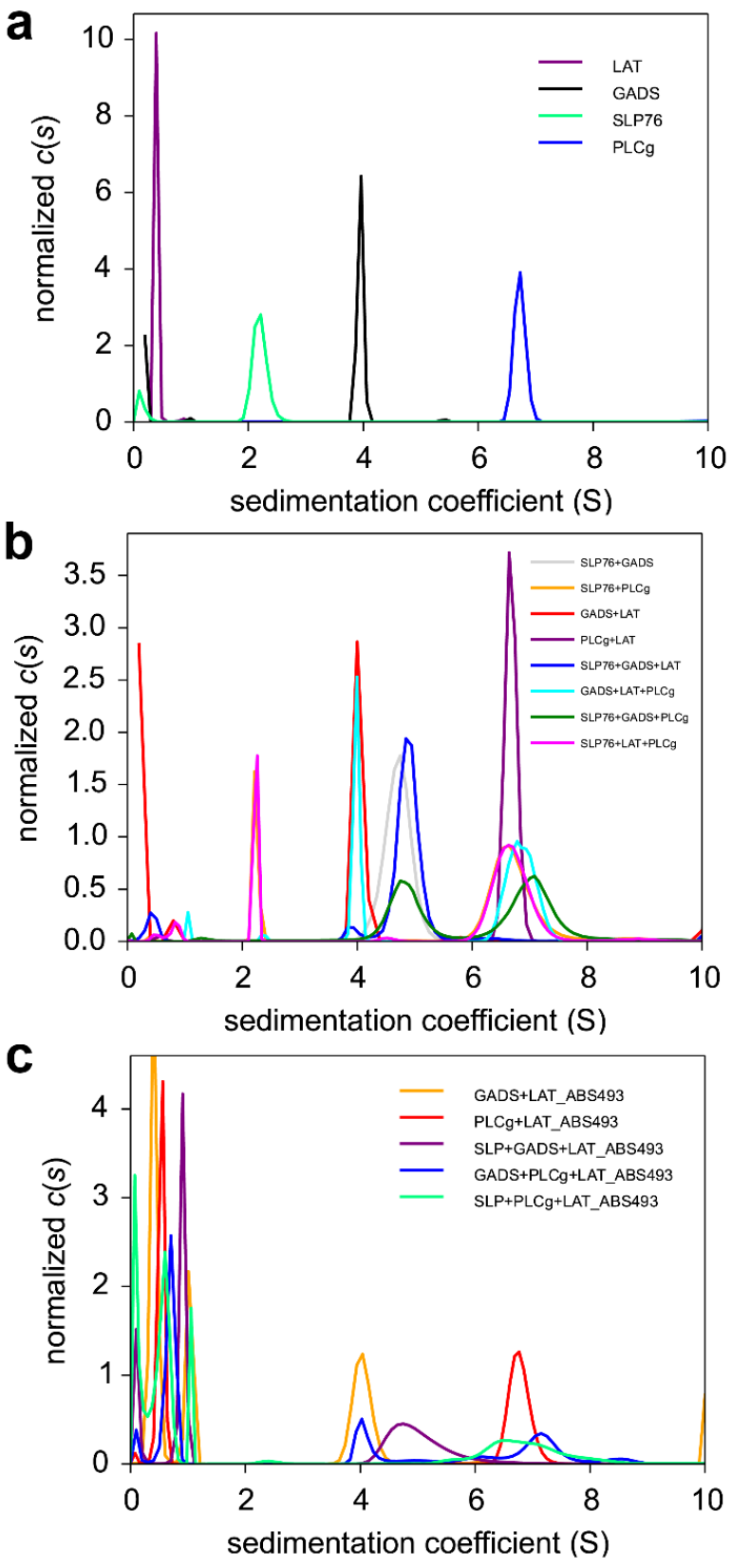
a
normalized c(s)
sedimentation coefficient (S)
LAT
GADS
SLP76
PLCg
b
normalized c(s)
sedimentation coefficient (S)
SLP76+GADS
SLP76+PLCg
GADS+LAT
PLCg+LAT
SLP76+GADS+LAT
GADS+LAT+PLCg
SLP76+GADS+PLCg
SLP76+LAT+PLCg
c
normalized c(s)
sedimentation coefficient (S)
GADS+LAT_ABS493
PLCg+LAT_ABS493
SLP+GADS+LAT_ABS493
GADS+PLCg+LAT_ABS493
SLP+PLCg+LAT_ABS493

Figure S4: **SV-AUC control experiments for individual proteins and complex formation of SLP-76$_{tr-405}$, Halo-GADS$_{FL-646}$, pLAT$_{488}$, and PLC-γ1$_{FL}$.** Proteins were equimolar 2.5 µM in PBS, 1 mM EDTA 2.5 mM DTT, sedimenting at 50,000 rpm, 20 °C. Absorbance data at different wavelengths and interference data are simultaneously collected and converted to sedimentation coefficient distributions *c(s)*. **a,** Superposition of *c(s)* distributions from experiments of the individual components acquired by interference optics, showing SLP-76$_{tr-405}$ (green), Halo-GADS$_{FL-646}$ (black), PLC-γ1$_{FL}$ (blue), and pLAT$_{488}$ (purple). **b,** Based on interference optical detection, binary mixtures of SLP-76$_{tr-405}$ and Halo-GADS$_{FL-646}$ (grey), SLP-76$_{tr-405}$ and PLC-γ1$_{FL}$ (orange; virtually superimposed by the magenta line), Halo-GADS$_{FL-646}$ and pLAT$_{488}$ (red), PLC-γ1$_{FL}$ and pLAT$_{488}$ (purple); and ternary mixtures SLP-76$_{tr-405}$ with Halo-GADS$_{FL-646}$ and pLAT$_{488}$ (blue), Halo-GADS$_{FL-646}$ with pLAT$_{488}$ and PLC-γ1$_{FL}$ (cyan), SLP-76$_{tr-405}$ with Halo-GADS$_{FL-646}$ and PLC-γ1$_{FL}$ (green), and SLP-76$_{tr-405}$ with pLAT$_{488}$ and PLC-γ1$_{FL}$ (magenta). **c,** Based on absorbance detection at 493 nm showing only pLAT$_{488}$ and its complexes, mixtures of pLAT$_{488}$ with Halo-GADS$_{FL-646}$ (orange), with PLC-γ1$_{FL}$ (red), with SLP-76$_{tr-405}$ and Halo-GADS$_{FL-646}$ (purple), with Halo-GADS$_{FL-646}$ and PLC-γ1$_{FL}$ (blue), and with SLP-76$_{tr-405}$ and PLC-γ1$_{FL}$ (cyan), respectively.

Figure S5:

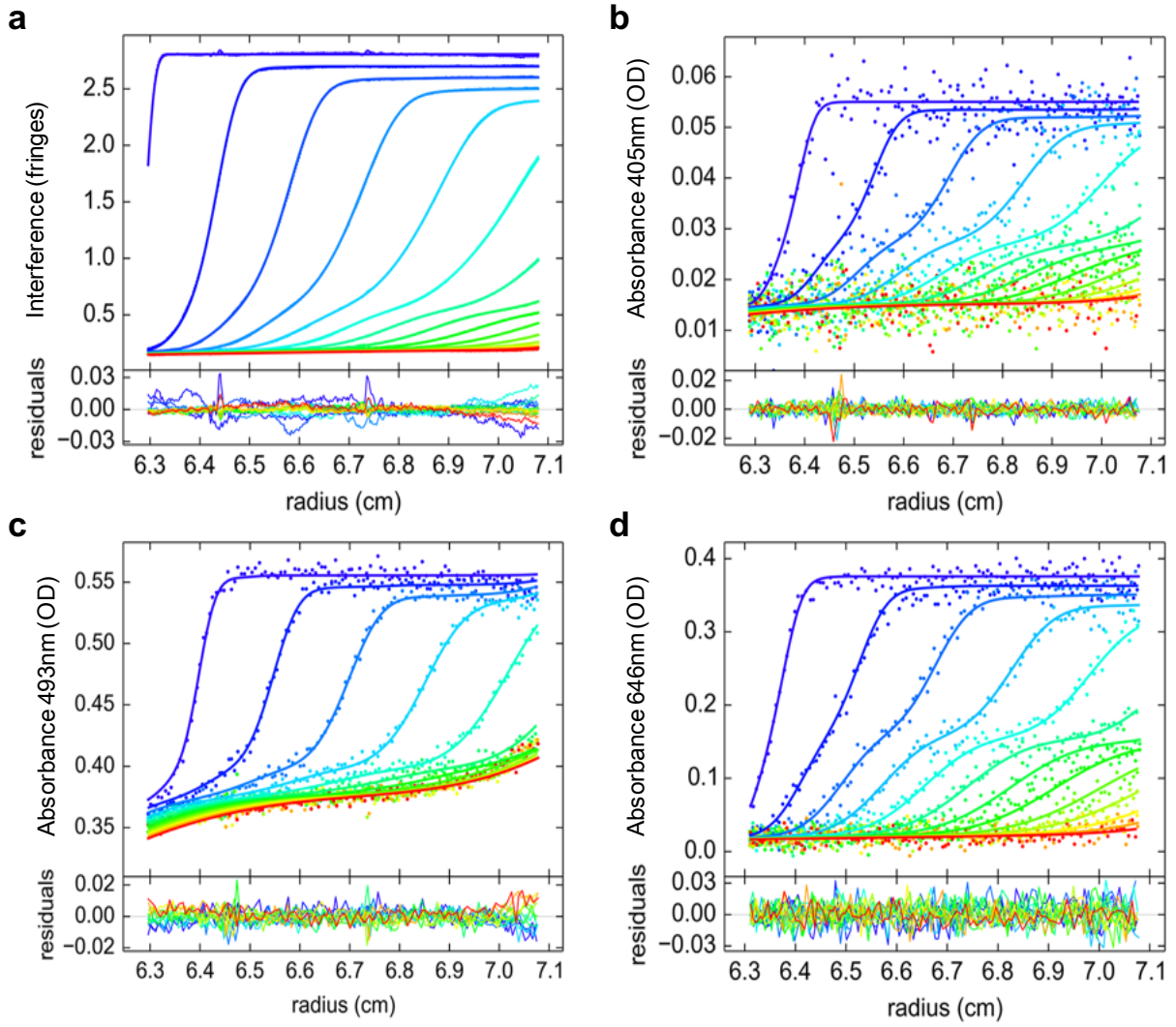

Figure S5: As representative example for the analysis raw sedimentation data, **sedimentation velocity boundary profiles of the quadruple mixture at 2.5 µM** (data in Figure 2) for interference signal (a), SLP-76 signal (b), LAT signal (c), and GADS signal (d).

Figure S6:

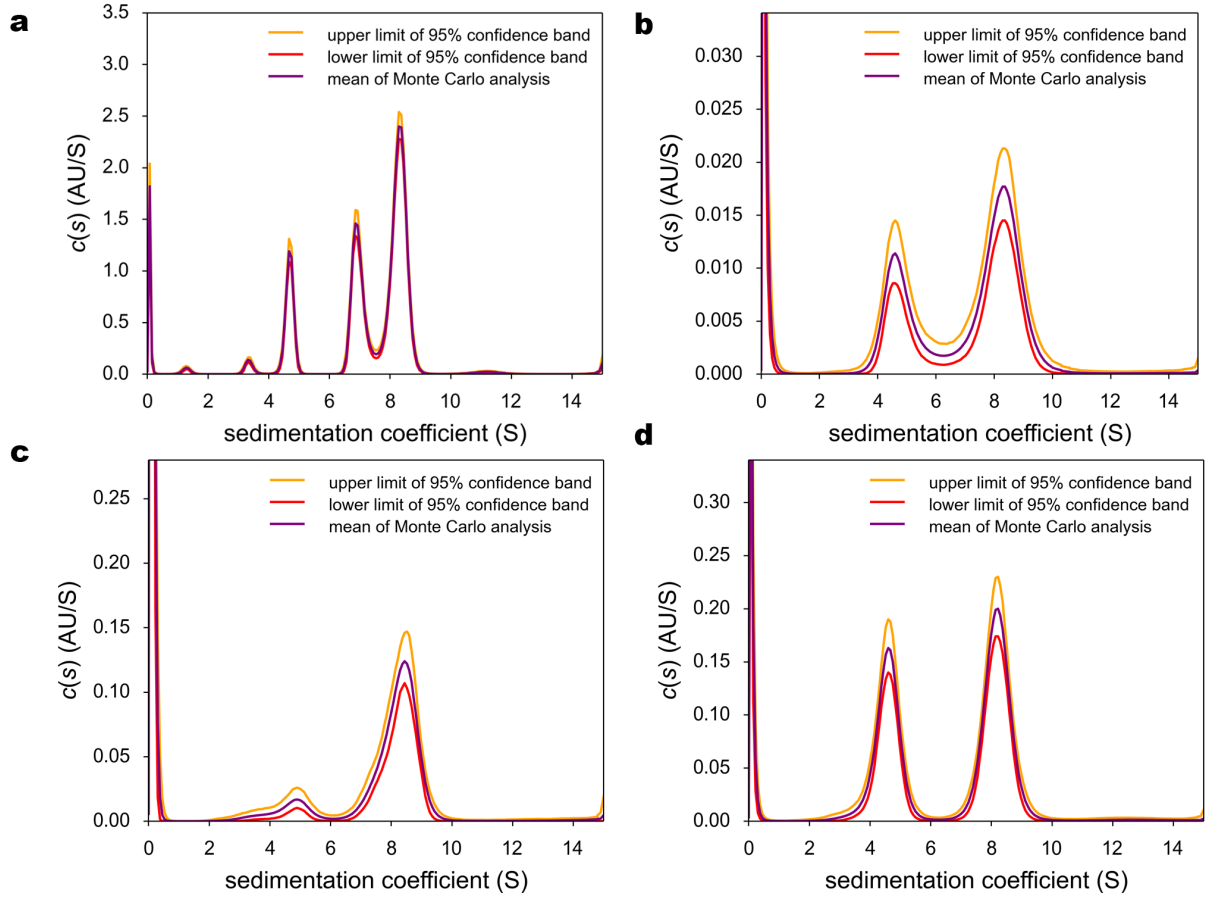

Figure S6: **Monte Carlo analysis on the c(s) distributions of the quadruple mixture at 2.5 µM** (data in Figure 2) for interference signal (a), SLP-76 signal (b), LAT signal (c), and GADS signal (d). For each panel, shown are the mean distribution of 1000 Monte Carlo iterations (purple), and the upper (orange) and lower (red) limit of the 95% confidence band. Statistical confidence intervals of the signal weighted-average *s*-values of the largest peak of interest were determined and resulted in the mean of 8.28 (±0.07%) S comprising a signal of 1.46 (±0.62%) fringes (a); 8.27 (±0.91%) S with a signal of 0.027 (±2.6%) OD (b); 8.25 (±0.32%) S with a signal of 0.16 (±1.3%) OD (c); and 8.19 (±0.40%) S with a signal of 0.21 (±1.4%) OD (d), respectively.

Figure S7:

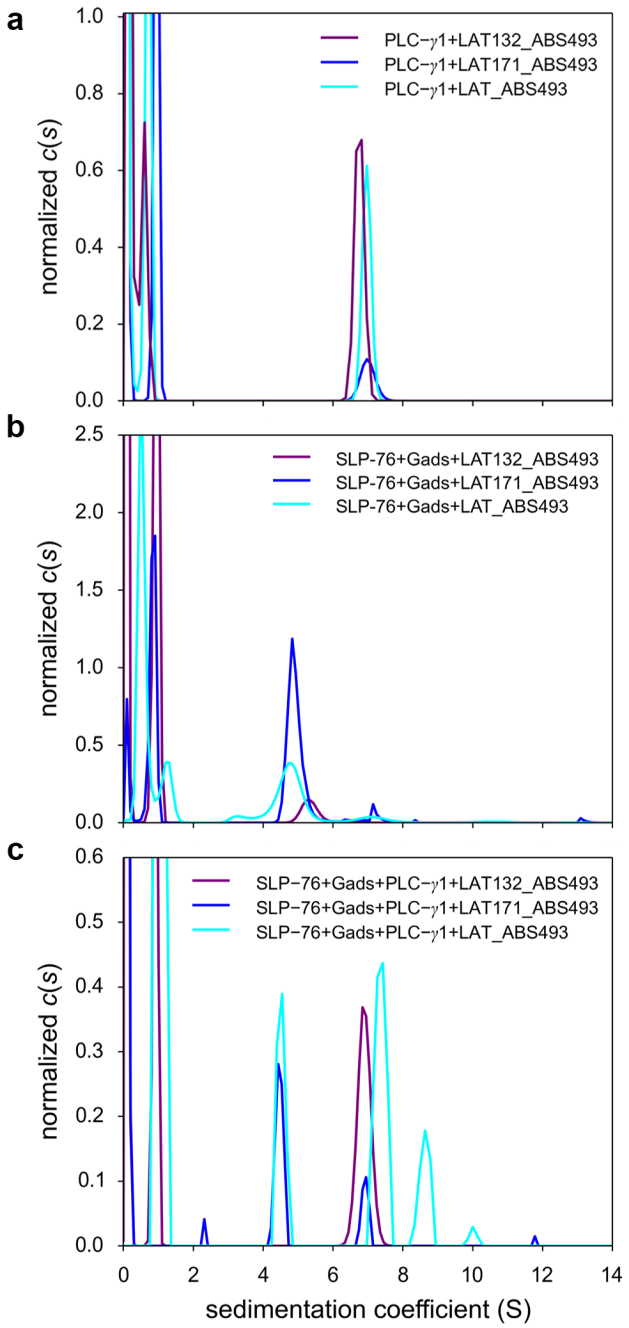

Figure S7: **SV-AUC analysis of protein complex formation of SLP-76$_{tr-405}$, Halo-GADS$_{FL-646}$, PLC-γ1$_{FL}$ with three forms of LAT, either doubly phosphorylated pLAT$_{488}$, (indicated as LAT) (cyan) or singly phosphorylated pLAT171$_{488}$ (blue) or pLAT132$_{488}$ (purple), monitored for LAT signal with absorbance detection at 493 nm**. All LAT peptides are labeled with Dylight-488. pLAT$_{488}$ is doubly phosphorylated at Y132 and Y171 position whereas, pLAT171$_{488}$ and pLAT132$_{488}$ are singly phosphorylated at position Y171 and Y132, respectively. Protein samples were equimolar mixture at 2.5 µM which were studied under the same condition as the ones shown in Figure 2. (a) binary mixtures of LAT peptides . (b) ternary mixtures

of LAT peptides with SLP-$76_{tr\text{-}405}$ and Halo-$GADS_{FL\text{-}646}$. (c) quaternary mixtures of LAT peptides with SLP-$76_{tr\text{-}405,}$ Halo-$GADS_{FL\text{-}646}$ and PLC-$\gamma1_{FL}$.

Figure S8:

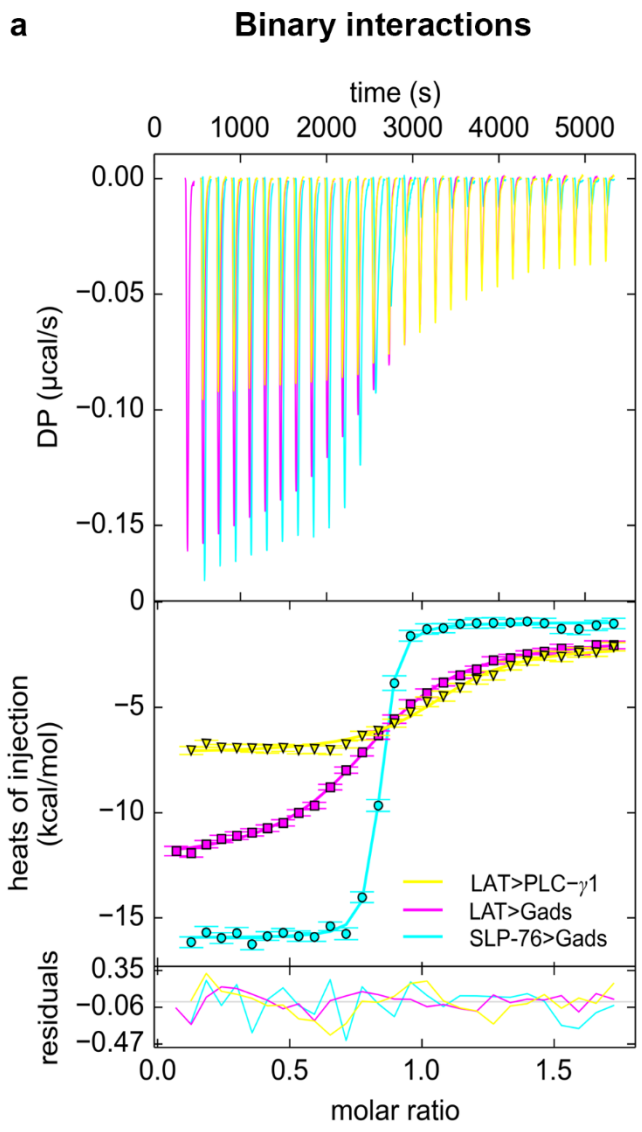
a
Binary interactions
time (s)
0
1000
2000
3000
4000
5000
0.00
−0.05
−0.10
−0.15
0
DP (µcal/s)
−5
−10
−15
heats of injection (kcal/mol)
LAT>PLC−γ1
LAT>Gads
SLP-76>Gads
0.35
−0.06
−0.47
residuals
0.0
0.5
1.0
1.5
molar ratio

b

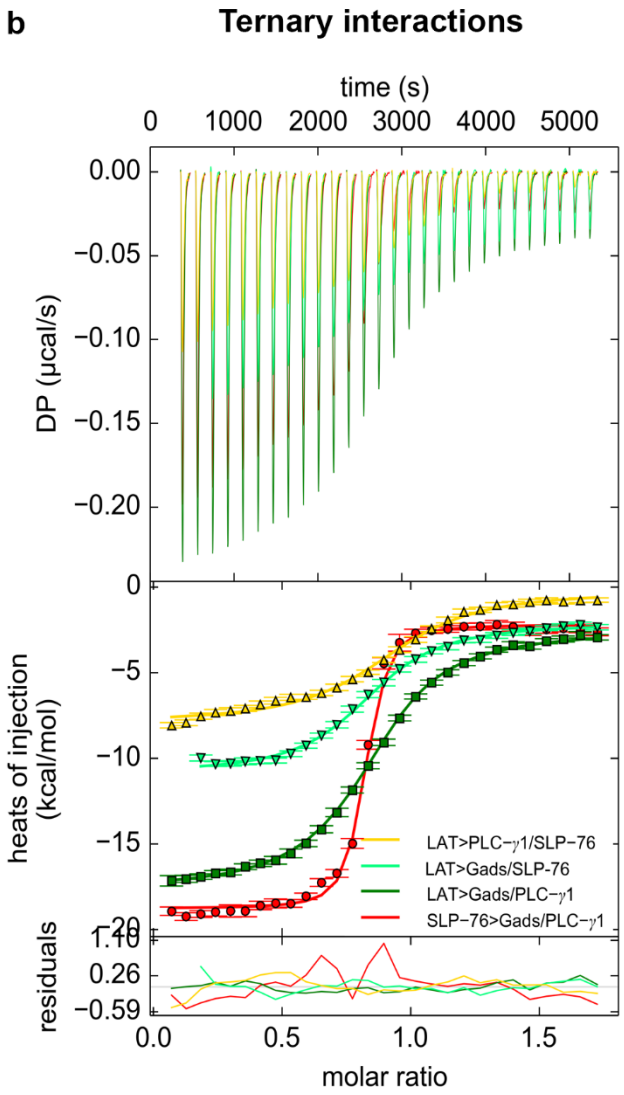
Ternary interactions
time (s)
0
1000
2000
3000
4000
5000
DP (µcal/s)
0.00
−0.05
−0.10
−0.15
−0.20
heats of injection (kcal/mol)
0
−5
−10
−15
−20
LAT>PLC−γ1/SLP−76
LAT>Gads/SLP-76
LAT>Gads/PLC−γ1
SLP−76>Gads/PLC−γ1
residuals
1.10
0.26
−0.59
0.0
0.5
1.0
1.5
molar ratio

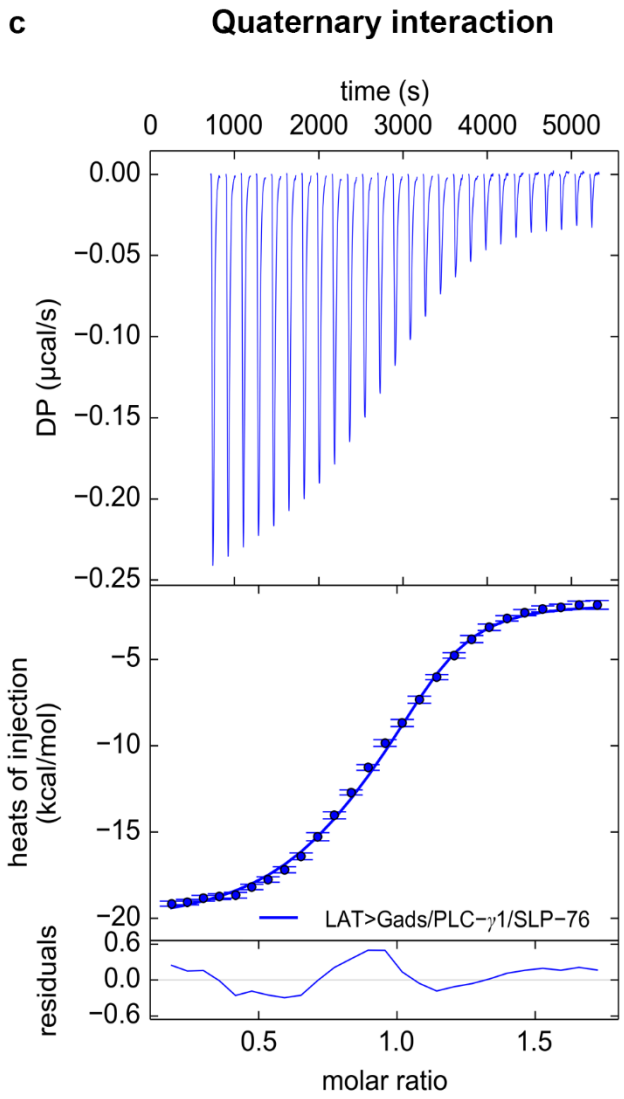

Figure S8: **Systematic exploration of the energetics of all binary, ternary, and quaternary complexes by ITC.** All experiments were done at 20°C in PBS, 1 mM EDTA, 2.5 mM DTT, with proteins indicated in the panel headers. For complexes containing pLAT, the phosphopeptide was taken into the syringe at a concentration of 50 µM with the binding partners in the cell equimolar at 5 µM. For complexes not containing LAT, SLP-76$_{tr}$ was loaded into the syringe at 40 µM, with binding partners in the cell equimolar at 4 µM. **a**, superposition of data from binary interactions measured for pLAT titrated into PLC-γ1$_{tr}$ (yellow), pLAT into Halo-Gads$_{FL}$ (magenta) and SLP-76$_{tr}$ into Halo-Gads$_{FL}$ (cyan). The thermodynamic parameters are given in the Table 1. **b**, superposition of data from all ternary interactions, each measured with equilibrated binary mixture in the cell and titrated with the third component: pLAT into a PLC-γ1$_{tr}$/SLP-76$_{tr}$ mixture (orange), pLAT into a Halo-Gads$_{FL}$/SLP-76$_{tr}$ mixture (light green), pLAT into a PLC-γ1$_{tr}$/Halo-Gads$_{FL}$ mixture (green), and SLP-76$_{tr}$ into a Halo-Gads$_{FL}$ /PLC-γ1$_{tr}$ mixture (red). In **c,** a mixture of Halo-Gads$_{FL}$ /PLC-γ1$_{tr}$/ SLP-76$_{tr}$ prequlibrated in the cell was titrated with pLAT (blue). For cooperativity factors of ternary and quaternary interactions see Table 2.

Figure S9:

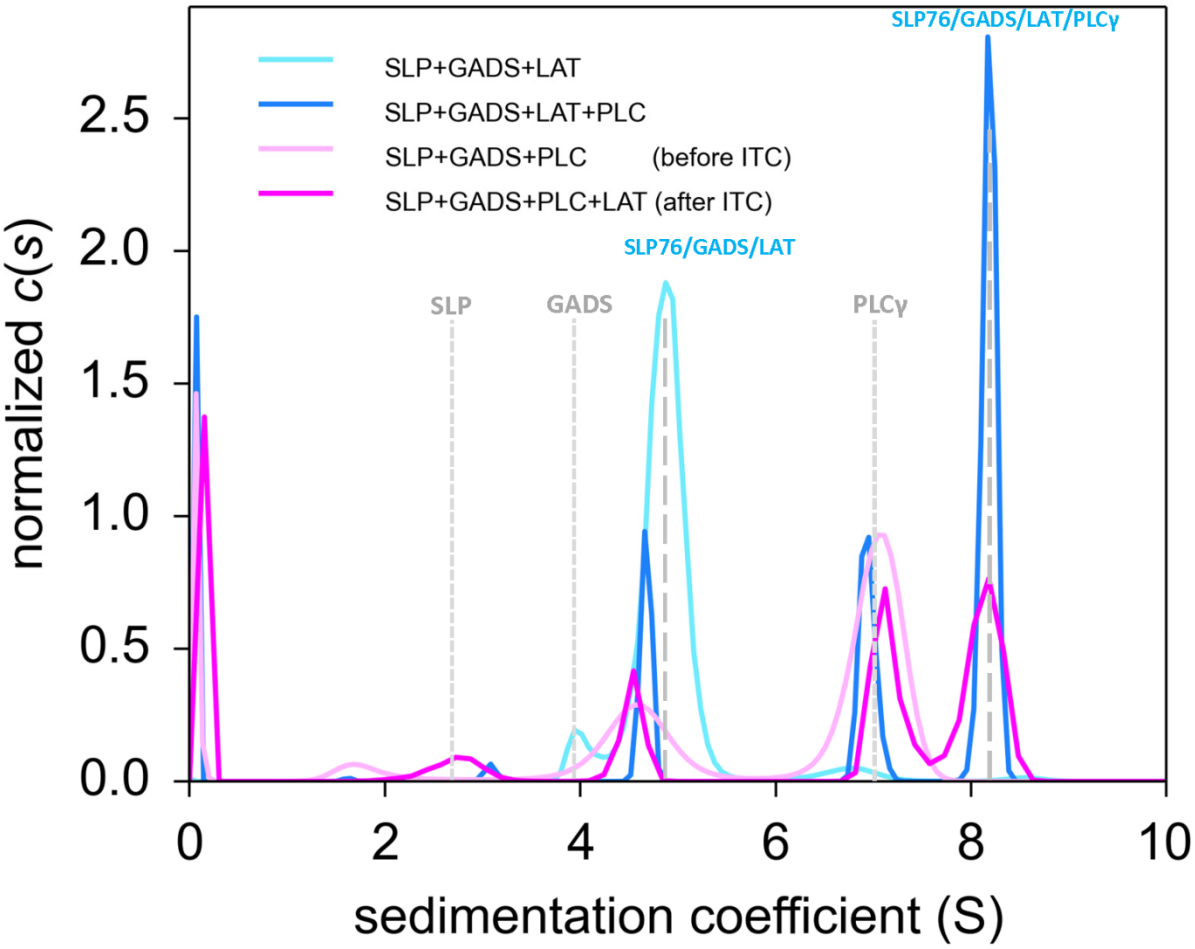

Figure S9: **Example for SV-AUC control experiments from samples recovered after ITC.** The sample of SLP-76_{tr}. Halo-$Gads_{FL}$, and PLC-$\gamma1_{FL}$ at 5µM in the ITC cell prior to the titration (light magenta) exhibits major peaks corresponding to the SLP-76_{Fl}/Halo-$Gads_{FL}$ complex and free PLC-$\gamma1_{FL}$. After the ITC titration with 50µM pLAT during the ITC experiment up to a molar ratio of ≈2:1 pLAT: SLP-76_{tr}/Halo-$Gads_{FL}$/PLC-$\gamma1_{FL}$, the sample was recovered from the cell and subjected to SV-AUC, yielding the *c(s)* distribution shown in magenta. Peaks corresponding to the SLP-76_{tr}/Halo-$Gads_{FL}$/PLC-$\gamma1_{FL}$/pLAT complex, in addition to excess free PLC-$\gamma1_{FL}$ and some SLP-76_{tr}/Halo-$Gads_{FL}$ complex are evident. Distributions from separate SV-AUC experiments with SLP-76_{tr}/Halo-$Gads_{FL}$/pLAT (cyan) and SLP-76_{tr}/Halo-$Gads_{FL}$/pLAT/PLC-$\gamma1_{FL}$ experiments (2.5 µM) are shown for reference.

Figure S10:

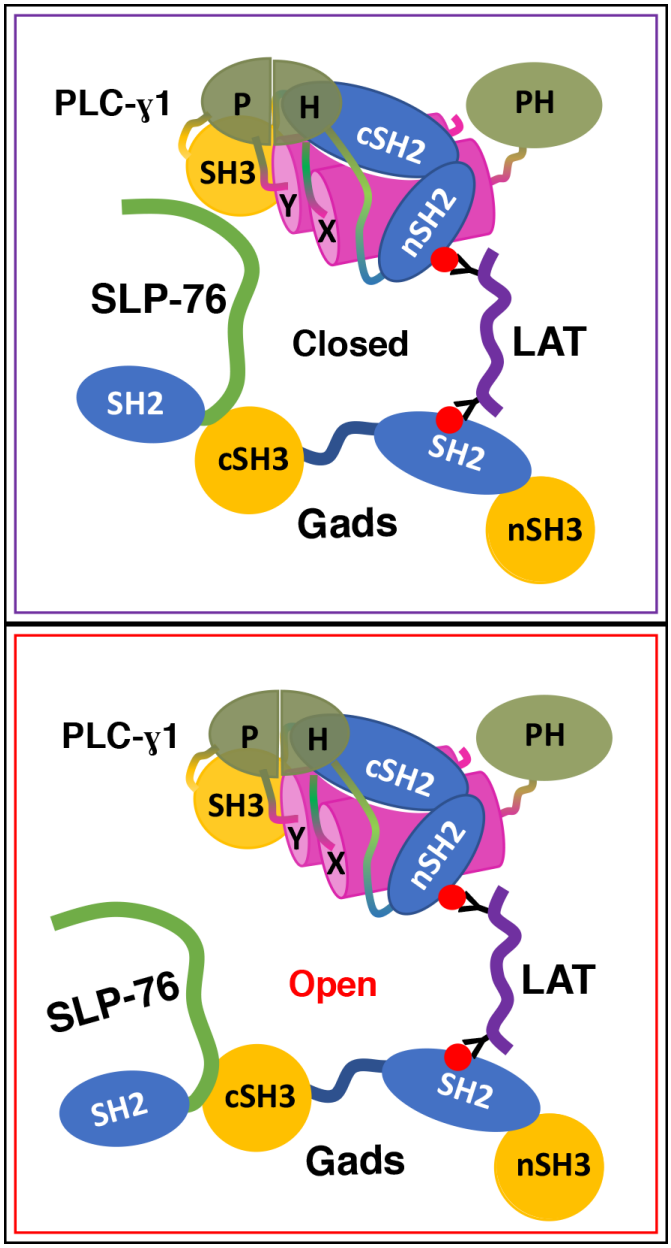

Figure S10: **Model of the SLP-76$_{tr}$/Halo-Gads$_{FL}$/pLAT/PLC-γ1$_{FL}$ quatenary complex model.** The proteins domains are represented in different colors and the interacting interfaces are shown, either in closed conformation (above) or in open conformation (below).

Supplementary Methods

Coupled reactions in the four-component mixture

In mixtures of LAT, Gads, PLC-γ1, and SLP-76 there are four binary interactions, four potential triple ternary interactions, and one quaternary interaction. Even though in practice not all interactions turn out to be strong or measurable they are all considered in the mathematical model with their appropriate affinity constants. In the following, *c* denotes the molar concentrations. We use subscripts L, G, P, and S to designate LAT, Gads, PLC-γ1, and SLP-76, respectively, and combinations of subscripts to denote their complexes.

The binary interactions are:

(1) LAT and Gads form a LAT/Gads complex following the mass action law

$$c_{LG} = K_{LG} c_L c_G \qquad \text{(Eq. 1)}$$

with equilibrium constant K_{LG}.

(2) Gads and SLP-76 form a Gads/SLP-76 complex following the mass action law

$$c_{GS} = K_{GS} c_G c_S \qquad \text{(Eq. 2)}$$

with equilibrium constant K_{GS}.

(3) SLP-76 and PLC-γ1 form a SLP-76/PLC-γ1 complex following the mass action law

$$c_{SP} = K_{SP} c_S c_P \qquad \text{(Eq. 3)}$$

with equilibrium constant K_{SP}.

(4) PLC-γ1 and LAT form a PLC-γ1/LAT complex following the mass action law

$$c_{PL} = K_{PL} c_P c_L \qquad \text{(Eq. 4)}$$

with equilibrium constant K_{PL}.

The ternary interactions are:

(5) LAT, Gads and SLP-76 form a LAT/Gads/SLP-76 triple complex following the mass action law

$$c_{LGS} = K_{LGS} c_L c_G c_S \qquad \text{(Eq. 5)}$$

with the cumulative equilibrium constant K_{LGS}. The latter may be expressed by binary equilibrium constants and a cooperativity constant $\alpha_{LGS} = K_{LGS}/(K_{LG} \times K_{GS})$.

(6) Gads, SLP-76, and PLC-γ1 form a Gads/SLP-76/PLC-γ1 triple complex following the mass action law

$$c_{GSP} = K_{GSP} c_G c_S c_P \qquad \text{(Eq. 6)}$$

with equilibrium constant K_{GSP}, which may expressed with a cooperativity constant $\alpha_{GSP} = K_{GSP}/(K_{GS} \times K_{SP})$.

(7) SLP-76, PLC-γ1, and LAT form a SLP-76/PLC-γ1/LAT triple complex following the mass action law

$$c_{SPL} = K_{SPL} c_S c_P c_L \quad \text{(Eq. 7)}$$

with equilibrium constant K_{SPL}, which may be expressed with a cooperativity constant $\alpha_{SPL} = K_{SPL}/(K_{SP} \times K_{PL})$.

(8) PLC-γ1, LAT, and Gads forming a PLC-γ1/LAT/Gads triple complex following the mass action law

$$c_{PLG} = K_{PLG} c_P c_L c_G \quad \text{(Eq. 8)}$$

with equilibrium constant K_{PLG}, which may be expressed with a cooperativity constant $\alpha_{PLG} = K_{PLG}/(K_{PL} \times K_{LG})$.

The quaternary interaction is:

(9) LAT, Gads, SLP-76 and PLC-γ1 form a LAT/Gads/PLC-γ1/SLP-76 quadruple complex following the mass action law

$$c_{LGSP} = K_{LGSP} c_L c_G c_S c_P \quad \text{(Eq. 9)}$$

with equilibrium constant K_{LGSP}. It may be expressed as a total cooperativity constant $\alpha_{LGSP} = K_{LGSP}/(K_{LG} \times K_{GS} \times K_{SP} \times K_{PL})$, and further divided into an incremental cooperativity constant for ring closure $\Delta\alpha_{LGSP} = \alpha_{LGSP}/(\alpha_{LGS} \times \alpha_{GSP} \times \alpha_{SPL} \times \alpha_{PLG})$.

Conservation of mass requires that the total protomer concentrations, whether free or in complex, add up to the total concentrations:

$$c_{Ltot} = c_L + c_{LG} + c_{PL} + c_{LGS} + c_{SPL} + c_{PLG} + c_{LGSP} \quad \text{(Eq. 10)}$$

$$c_{Gtot} = c_G + c_{LG} + c_{GS} + c_{LGS} + c_{GSP} + c_{PLG} + c_{LGSP} \quad \text{(Eq. 11)}$$

$$c_{Stot} = c_S + c_{GS} + c_{SP} + c_{LGS} + c_{GSP} + c_{SPL} + c_{LGSP} \quad \text{(Eq. 12)}$$

$$c_{Ptot} = c_P + c_{SP} + c_{PL} + c_{GSP} + c_{SPL} + c_{PLG} + c_{LGSP} \quad \text{(Eq. 13)}$$

Given all equilibrium binding constants K_{LG}, K_{GS}, K_{SP}, K_{PL}, K_{LGS}, K_{GSP}, K_{SPL}, K_{PLG}, K_{LGSP}, and the total concentrations c_{Ltot}, c_{Gtot}, c_{Stot}, c_{Ptot}, simultaneous solutions to Eqs. 1-13 are calculated in SEDPHAT, with a numerical accuracy of $10^{-6} c_{tot}$ or better for all components. This provides molar concentrations of all free species and all complexes, which can be used, in turn, to model measured heats of binding and weight-average sedimentation coefficients along experimental titration series in ITC and SV, respectively.

Standard free energy of binding and cooperativity

Binding constants relate to the standard free energy of binding as

$$\Delta G^0 = -RT \ln K \qquad \text{(Eq. 14)}$$

For example, for the quadruple complex the total free energy of binding is

$$-\frac{\Delta G^0_{LGSP}}{RT} = \ln \frac{c_{LGSP}}{c_L c_G c_S c_P} = \ln K_{LGSP} \qquad \text{(Eq. 15)}$$

The definition of the overall cumulative cooperativity constant of the quaternary complex $\alpha_{LGSP} = K_{LGSP}/(K_{LG} \times K_{GS} \times K_{SP} \times K_{PL})$ corresponds to a subdivision of the total free energy of binding

$$-\frac{\Delta G^0_{LGSP}}{RT} = \ln K_{LGSP} = \ln \frac{\alpha_{LGSP}}{K_{LG} K_{GS} K_{SP} K_{PL}} = \ln \alpha_{LGSP} - \ln K_{LG} - \ln K_{GS} - \ln K_{SP} - \ln K_{PL} \qquad \text{(Eq. 16)}$$

or

$$\Delta G^0_{LGSP} = \Delta G^0_{LG} + \Delta G^0_{GS} + \Delta G^0_{SP} + \Delta G^0_{PL} + \Delta\Delta G^0_{LGSP} \qquad \text{(Eq. 17)}$$

where

$$\Delta\Delta G^0_{LGSP} = -RT \ln \alpha_{LGSP} = \Delta G^0_{LGSP} - \left(\Delta G^0_{LG} + \Delta G^0_{GS} + \Delta G^0_{SP} + \Delta G^0_{PL} \right) \qquad \text{(Eq. 18)}$$

The further decomposition of the cumulative cooperativity of the quaternary complex into contributions from ternary interactions and ring closure, defined as $\Delta\alpha_{LGSP} = \alpha_{LGSP}/(\alpha_{LGS} \times \alpha_{GSP} \times \alpha_{SPL} \times \alpha_{PLG})$ leads to

$$\Delta\Delta G^0_{LGSP} = -RT \ln \left(\Delta\alpha_{LGSP} + \alpha_{LGS} + \alpha_{GSP} + \alpha_{SPL} + \alpha_{PLG} \right) \qquad \text{(Eq. 19)}$$

and corresponds to the definition of an incremental free energy of ring closure

$$\Delta\Delta\Delta G_{LGSP}{}^0 = \Delta G^0_{LGSP} - \left(\Delta G^0_{LG} + \Delta G^0_{GS} + \Delta G^0_{SP} + \Delta G^0_{PL} \right) - \left(\Delta\Delta G^0_{LGS} + \Delta\Delta G^0_{GSP} + \Delta\Delta G^0_{SPL} + \Delta\Delta G^0_{PLG} \right) \qquad \text{(Eq. 20)}$$

where $\Delta\Delta G$ contributions from the triple complexes are analogously defined.

For clarity, a different notation is used in the main text of the paper, omitting the superscript zeros and referring to $\Delta\Delta\Delta G_{LGSP}$ simply as $\Delta\Delta G_{quad}$. The same subdivisions of the free energy are applied to their enthalpic and entropic components.